

Suppression of Circulating Current in Paralleled Inverters with Isolated DC-link

Hyun-Sam Jung*, Jeong-Mock Yoo*, Seung-Ki Sul*, Hak-Jun Lee**, Chanook Hong**

* Seoul National University

School of Electrical Engineering & Computer Science, Seoul National University, 1 Gwanak-ro, Gwanak-gu, Seoul, Korea

** LSIS Co., Ltd.

Industrial Automation Business Group

Anyang-si

Kyeonggi-Do, Korea

hjleea@lsis.com, cohong@lsis.com

Abstract— In this paper, it is described how the circulating current flows between inverters which have isolated DC-link such as Cascaded H Bridge (CHB) topology, when they operating in parallel. In this case, Zero Sequence Circulating Current (ZSCC) flowing through shared DC-link cannot flow between inverters in parallel. However, circulating current is provoked by asynchronous switching instant of devices and difference of DC-link voltages of parallel inverters. The circulating current should be suppressed by sharing inductor which is inserted between inverters. Generally, all of the inverters should synthesize the same output voltage reference for load current control, to minimize the size of this sharing reactor. However, this conventional method cannot guarantee to diminish circulating current in the transient state and even in the steady state. In this paper, to reduce circulating current, after deriving circulating current model, circulating current control method is devised based on the model. This proposed algorithm is applied to Active Front End 5Level-CHB inverter system for medium voltage drive. Simulation and experimental results are provided to verify the effectiveness of the proposed control scheme.

Keywords—Parallel operation, Circulating current, Cascaded H-bridge

I. INTRODUCTION

By parallel operation, multiple inverters which have the same power capacity can be applicable to motor drive systems with various power capacities. It can make system be designed as modular structure. It may result in reduced production and maintenance cost of overall motor-drive system [1]-[3]. Besides, even if one of the inverters would fail, the motor still can be driven continuously with reduced power capacity. It enhances system reliability. Due to these advantages, parallel operation of inverters has been applied to many industrial field, especially large medium voltage drives.

In the parallel operation of the inverters, there is always the possibility of circulating current between paralleled inverters. The circulating current not only increase the current rating of the inverter but also degrade efficiency of overall drive system. Most of the conventional researches on circulating current control are limited to parallel operation with non-isolated DC-link of each inverter. In this case, due to common DC-link, a considerable amount of Zero Sequence Circulating Current (ZSCC) inevitably flows between inverters connected in parallel [4]-[8]. Many researches have been carried out on the ZSCC control. According to these researches, zero vector is utilized, to prevent ZSCC [9]-[11].

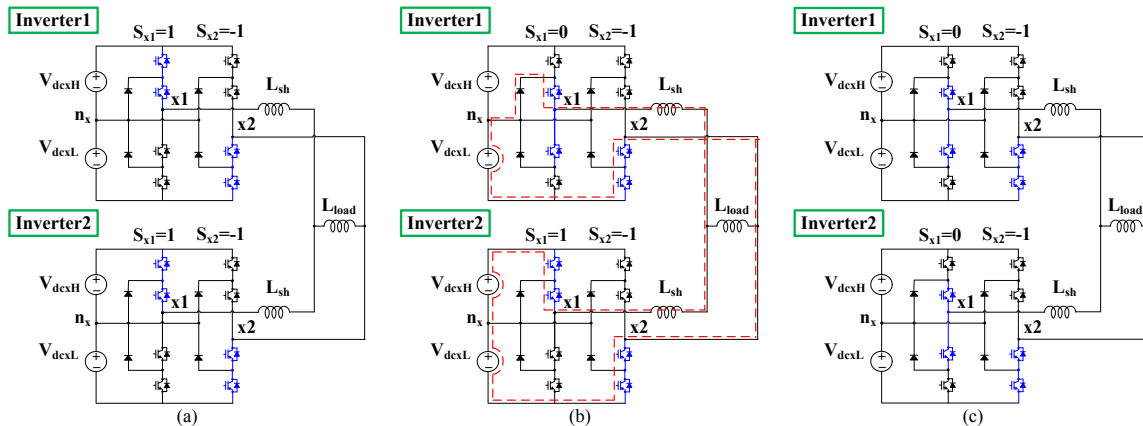


Fig. 1: Example of circulating current provoked by changing switching state asynchronously

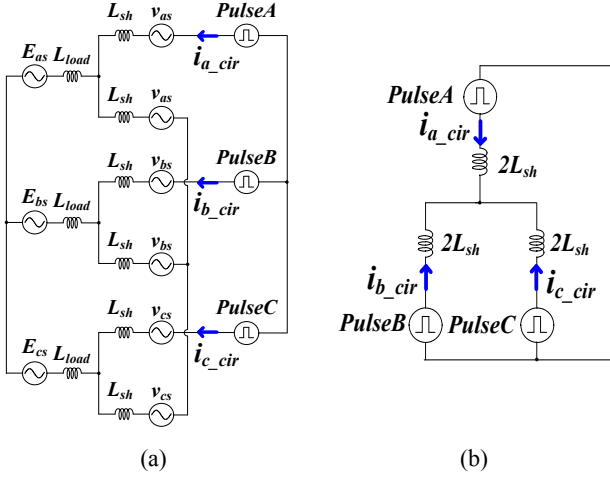


Fig. 2: Equivalent circuit of circulating current

In case of CHB which is the most widely employed as circuit topology in Medium Voltage (MV) drive, cells are connected in cascade. Also, each cell has an isolated DC-link because converters on the grid side in the cell are fed by isolated AC source through multi-winding input transformer. It means that ZSCC can't flow, when this kind of system operates in parallel. Besides, the inverters should synthesize the same output voltage for load current control, in order to minimize the circulating current. However, even if all of inverters in parallel synthesize the same output voltage, their pole voltages would not be the same, because they are affected by modulation conditions such as turn on/off time delay of device, T_{on} , T_{off} , depending on its temperature, gate signal propagation delay, and DC-link voltage. As a result, differences of these conditions make circulating current flow between inverters in parallel.

In this paper, after analyzing the circulating current, equivalent circuit of circulating current is derived from the general case that arbitrary number of inverters are connected in parallel under appropriate assumptions. Based on this model, a control scheme to suppress the circulating current of paralleled CHB inverters is devised. Feasibility and validity of the devised method are confirmed by simulation and experimental results.

II. CIRCULATING CURRENT CONTROL

A. Circulating Current

Fig. 1 describes that a sequence of switching state changes in x-phase of inverters when two 5Level-CHB inverters on the load side operate in parallel, where x denotes an arbitrary phase among a, b, and c. S_{x1} and S_{x2} represent switching function of leg1 and leg2 in x phase, respectively. The switching function has three switching states. Three switching states are defined as follow, "1" states that pole voltage of its leg is V_{dcH} , "0" states that pole voltage of its leg is 0, "-1" states that pole voltage of its leg is $-V_{dcL}$. Fig. 1 shows that S_{x1} changes from 1 to 0. Fig. 1 (a) and Fig. 1 (c) show the switching state of the parallel inverters at the starting and the switching state at the final respectively under the assumption that there is slight time delay in switching of

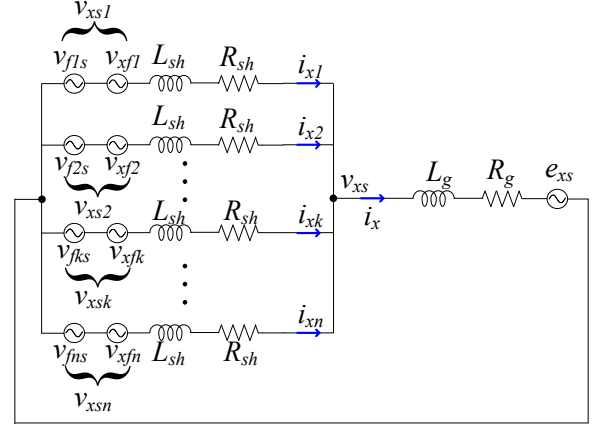


Fig. 3: X-phase model in n parallel operation of inverters

inverter 2 compared with that of inverter1. In Fig. 1 (b), where S_{x1} of inverters in parallel are different, S_{x1} of inverter1 changes from 1 to 0, before that of inverter 2 changes. This asynchronous switching state due to the different time delay of the gating signal and associated switching of the power semiconductor provokes circulating current like red dashed line in Fig. 1 (b) which shows conducting path of circulating current.

Output voltage of x-phase of inverter is represented as $V_{dc}/2 \times (S_{x1} - S_{x2})$, where V_{dc} denotes total DC-link voltage. Difference between output voltages of inverter1 and inverter2 varies like $0 \rightarrow V_{dcxH} \rightarrow 0$, when switching state is changed as shown in Fig. 1. It is worthy of note that the voltage source provoking the circulating current can be represented as voltage source with pulse shape. From this intuition, the maximum of circulating current can be derived. Fig. 2 (a) shows the equivalent circuit including the pulse voltage generated by the time delay, PulseX, and circulating current generated by the pulse voltage, i_{x_cir} . In order to analyze relationship between pulse voltage and the circulating current, if load side inductor, L_{load} , is considered as a current source, Fig. 2 (a) can be redrawn like Fig. 2 (b), by replacing voltage sources with short circuit and current sources with open circuit. In this system, the maximum pulse voltage is V_{dc} . From this simplified equivalent circuit, peak value of circulating current can be represented as (1), where T_{delay} is the maximum difference of switching time coming from difference of T_{on} , T_{off} , of device and propagation delay of gating signal.

$$i_{cir_x} = \frac{2V_{dc}}{3L_{sh}} T_{delay} \cdot \quad (1)$$

$$i_{cir_x} = \frac{2V_{dc}}{3L_{sh}} T_{delay}' + \frac{2V_{dc_diff}}{3L_{sh}} T_{samp} \cdot \quad (2)$$

Eq. (1) comes from Fig. 2 (b), where DC-link capacitors are considered as ideal voltage sources with the same value. However, in the real system, DC-link voltages of each inverter in parallel are neither the same value nor ideal voltage sources. If difference of DC-link voltage between inverters in parallel, V_{dc_diff} , is considered, circulating current can be described as (2) instead of (1), where T_{delay}' includes PWM delay induced by DC-link voltage difference.

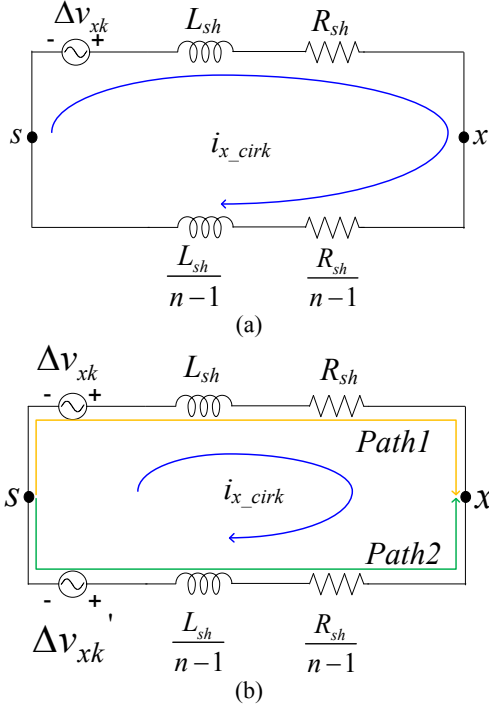


Fig. 4: x-phase model simplified equivalent model in case of n parallel operation of inverters

B. Circulating Current Model and Control Method

In this section, so as to suppress the circulating current, circulating current model is derived from n parallel operation of x-phase circuit, as shown in Fig.3. Based on this model, circulating current controller can be implemented.

By applying KVL to n branches connected in parallel like Fig.3, n equations are given as (3). Current conducting through k^{th} branch of x-phase, i_{xk} , is defined as sum of average current, i_{x_av} , and circulating current, i_{x_cir} , like (4), where average current is defined as (5). Sum of circulating currents becomes null from that of all of branch currents, as shown in (6). Sum of KVL equations, (3), can be rewritten as (7). If (8) is assumed,

average current model could be simplified like (9). This assumption is reasonable, because voltage drop of sharing inductor is small enough to be negligible. Also, it is desirable that inductance of the sharing inductor should be minimized.

Output phase voltage of k^{th} branch, v_{xsk} , is defined as sum of v_{xs} and difference voltage, Δv_{xk} , like (10). Eq. (11) is given by substituting (10) into v_{xsk} in (3). This equation means that the difference voltage is a degree of freedom to control circulating current directly. Therefore, v_{xsk} consists of two voltage components. One is the output voltage, v_{xs} , in order to control average current. The other is the difference voltage, Δv_{xk} , for controlling the circulating current. Eq. (12) is deduced by summing KVL equations, (3). Based on these equations, (9) and (11), both average current and circulating current would be controlled independently.

$$\begin{aligned} (v_{xs1} - e_{xs}) &= z_{sh}i_{x1} + z_{load} \left(\sum_{k=1}^n i_{xk} \right) \\ (v_{xs2} - e_{xs}) &= z_{sh}i_{x2} + z_{load} \left(\sum_{k=1}^n i_{xk} \right) \\ &\vdots \\ (v_{xsk} - e_{xs}) &= z_{sh}i_{xk} + z_{load} \left(\sum_{k=1}^n i_{xk} \right) \\ &\vdots \\ (v_{xsn} - e_{xs}) &= z_{sh}i_{xn} + z_{load} \left(\sum_{k=1}^n i_{xk} \right) \end{aligned} \quad (3)$$

$$\text{where, } Z_{sh} = R_{sh} + sL_{sh},$$

$$Z_{load} = R_{load} + sL_{load}.$$

$$i_{xk} = i_{x_av} + i_{x_cir}. \quad (4)$$

$$i_{x_av} = \frac{i_x}{n} = \frac{\sum_{k=1}^n i_{xk}}{n}. \quad (5)$$

$$\sum_{k=1}^n i_{x_cir} = 0. \quad (6)$$

TABLE I. EXAMPLE OF X PHASE COMPENSATION VOLTAGE OF EACH BRANCH WHICH IS IN N PARALLEL CASE

n=2	n=3	n=4
$\Delta v_{x1_comp} = \Delta v_{x1}$	$\Delta v_{x1_comp} = \Delta v_{x1} - 0.5\Delta v_{x2}$	$\Delta v_{x1_comp} = \Delta v_{x1} - \Delta v_{x2}/3 - \Delta v_{x3}/3$
$\Delta v_{x2_comp} = -\Delta v_{x1}$	$\Delta v_{x2_comp} = \Delta v_{x2} - 0.5\Delta v_{x1}$	$\Delta v_{x2_comp} = \Delta v_{x2} - \Delta v_{x1}/3 - \Delta v_{x3}/3$
$i_{x_av} = \frac{v_{xs} - e_{xs}}{z_{sh} + 2z_{load}}$	$\Delta v_{x3_comp} = -0.5\Delta v_{x1} - 0.5\Delta v_{x2}$	$\Delta v_{x3_comp} = \Delta v_{x3} - \Delta v_{x1}/3 - \Delta v_{x2}/3$
$i_{x1_cir} = i_{x1} - i_{x_av}$	$i_{x_av} = \frac{v_{xs} - e_{xs}}{z_{sh} + 3z_{load}}$	$\Delta v_{x4_comp} = -\Delta v_{x1}/3 - \Delta v_{x2}/3 - \Delta v_{x3}/3$
$i_{x2_cir} = -i_{x1_cir}$	$i_{x1_cir} = i_{x1} - i_{x_av}$	$i_{x_av} = \frac{v_{xs} - e_{xs}}{z_{sh} + 4z_{load}}$
	$i_{x2_cir} = i_{x2} - i_{x_av}$	$i_{x1_cir} = i_{x1} - i_{x_av}$
	$i_{x3_cir} = -i_{x1_cir} - i_{x2_cir}$	$i_{x2_cir} = i_{x2} - i_{x_av}$
		$i_{x3_cir} = i_{x3} - i_{x_av}$
		$i_{x4_cir} = -i_{x1_cir} - i_{x2_cir} - i_{x3_cir}$

$$\Sigma(v_{xsk} - e) = \Sigma(z_{sh} + nz_{load}) \times i_{x_av}. \quad (7)$$

$$\frac{\Sigma v_{xsk}}{n} = v_{xs}. \quad (8)$$

$$i_{x_av} = \frac{\frac{\Sigma v_{xsk} - e}{n}}{(z_{sh} + nz_{load})} \cong \frac{v_{xs} - e}{(z_{sh} + nz_{load})}. \quad (9)$$

If only voltage source of k^{th} branch to suppress the circulating current of k^{th} branch is considered, then x-phase model in Fig.3 can be simplified to Fig.4 (a). According to Fig.4 (a), difference between potential of two nodes, x and s, is induced by voltage dividing of Δv_{xsk} . In other words, this voltage source, Δv_{xsk} , can affect the output voltage, v_{xs} . To eliminate this influence on the output voltage, both additional voltage source, Δv_{xsk} , and another compensating voltage source, $\Delta v_{xsk}'$, will be added to equivalent circuit, as shown in Fig.4 (b). In the Fig. 4 (b), where path1 and path2 are defined, voltage following path 1 and path 2 are null by KVL, if both the additional voltages are defined as (13). As a result, if all of branches are considered by applying the superposition principle, total compensation voltage, Δv_{xk_comp} , is defined as (14).

Based on this scheme of the circulating current suppression, total equivalent control loop can be depicted as shown in Fig.5. From Fig.5, gains of circulating current controller can be set as (15), for this close loop function to be 1st-order Low Pass Filter

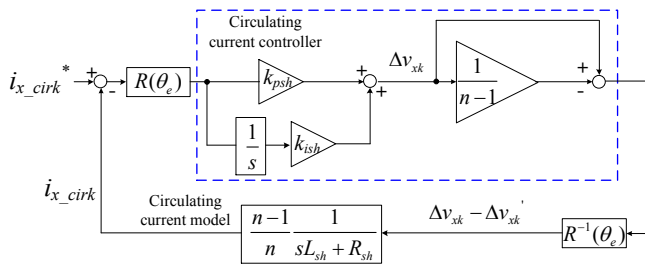


Fig. 5: Proposed circulating current controller based on the model of circulating current

TABLE II. SIMULATION PARAMETERS

Parameter	Value
Rated power	0.417 MW, 4 parallel
EMF	1720 Vrms, 60 Hz
Rated current	108 Arms, 4 parallel
R_{load}	0.4 Ω
L_{load}	6.2 mH
L_{sh}	60 uH
R_{sh}	11.6m Ω
Tdelay(Inv1, Inv2)	400 ns
Tdelay(Inv2, Inv3)	400 ns
Tdelay(Inv3, Inv1)	800 ns
Tdelay(Inv4, Inv1)	800 ns
C_{dc}	1800 uF

(LPF) with bandwidth, ω_{sh} . Table 1. shows examples, when n is equal to 2, 3, 4, respectively.

$$v_{xsk} = v_{xs} + \Delta v_{xk}. \quad (10)$$

$$\Delta v_{xk} = z_{sh} i_{x_cirk}. \quad (11)$$

$$\Sigma \Delta v_{xk} = 0. \quad (12)$$

$$\Delta v_{xk} = z_{sh} i_{x_cirk} \quad (13)$$

$$\Delta v_{xk}' = -\frac{z_{sh}}{n-1} i_{x_cirk} = -\frac{\Delta v_{xk}}{n-1}.$$

$$\Delta v_{xk_comp} = \Delta v_{xk} - \frac{1}{n-1} \sum_{i \neq k} \Delta v_{xi}. \quad (14)$$

$$k_{psh} = \omega_{sh} L_{sh} \quad (15)$$

$$k_{ish} = \omega_{sh} R_{sh}$$

III. SIMULATION RESULT

Simulation is conducted with MATLAB to verify the circulating current model and proposed control method. In the simulation, 4 parallel Active Front End 5Level-CHB(AFE 5L-CHB) inverter is employed for current control in R-L load with 1720V, 60Hz, ideal voltage source. These parameters are deduced from 1.67MW induction machine drive system and listed in Table II. Simulation configuration is shown in Fig. 6.

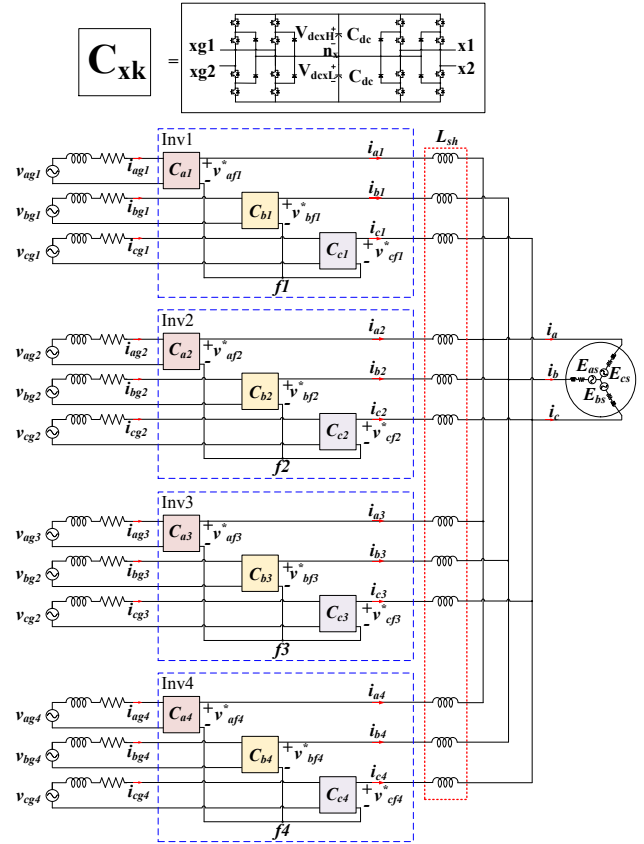


Fig. 6: Simulation model: 4 parallel AFE 5L-CHB

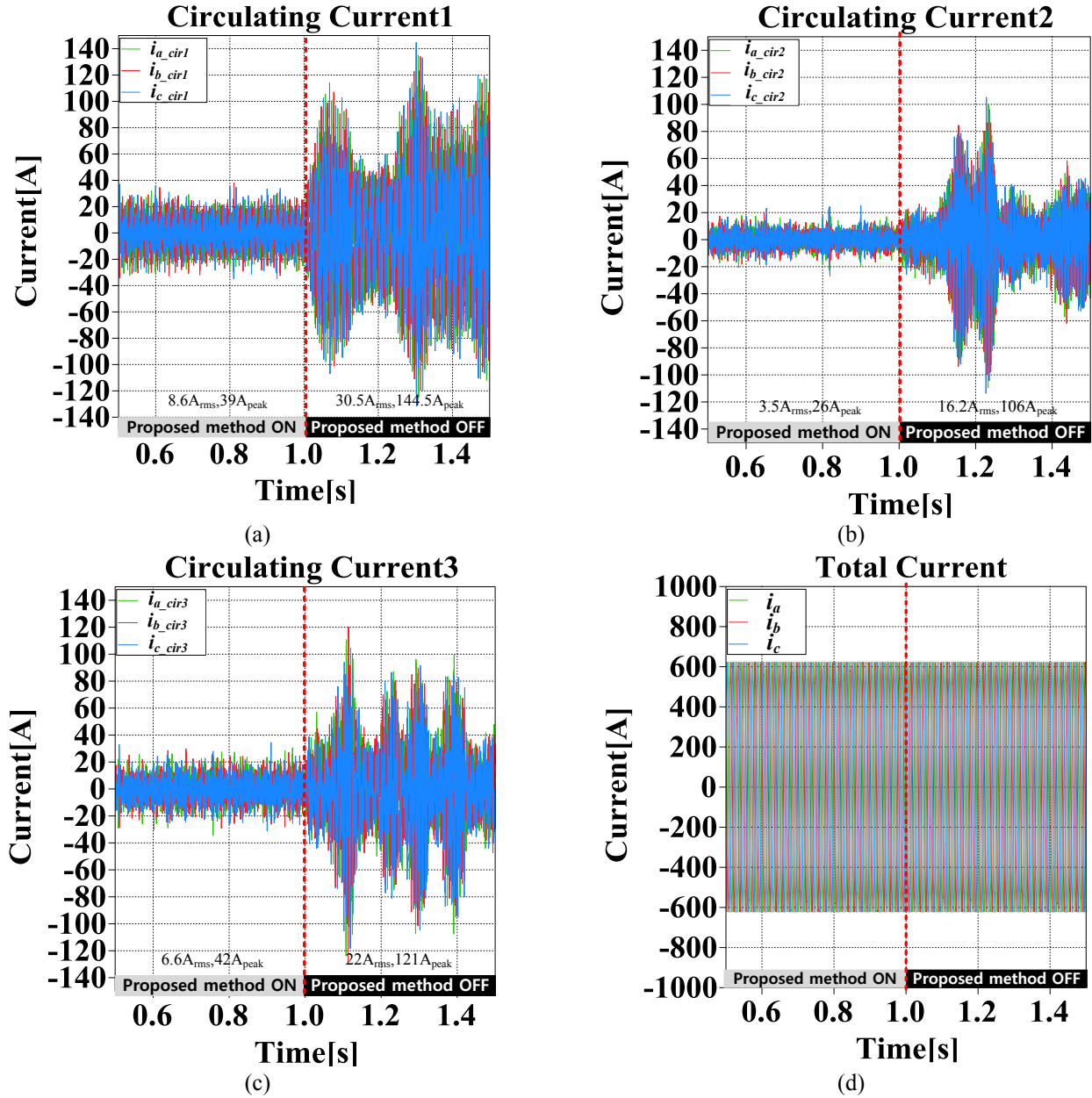


Fig. 7: Simulation results: (a) i_{abc_cir1} , (b) i_{abc_cir2} , (c) i_{abc_cir3} , (d) total current, i_{abc}

To show validity and effectiveness of the proposed suppression method, the proposed circulating current controller is engaged from 0.5s to 1s and disengaged after 1s.

Fig. 7 shows simulation results. When the proposed method is engaged, the circulating current of Inv1, Inv2, Inv3 and Inv4 are well regulated under $10A_{rms}$, $50A_{peak}$. However, after disengagement of the controller at 1s, RMS and maximum of circulating current increase by about 300% or 400%.

IV. EXPERIMENTAL RESULT

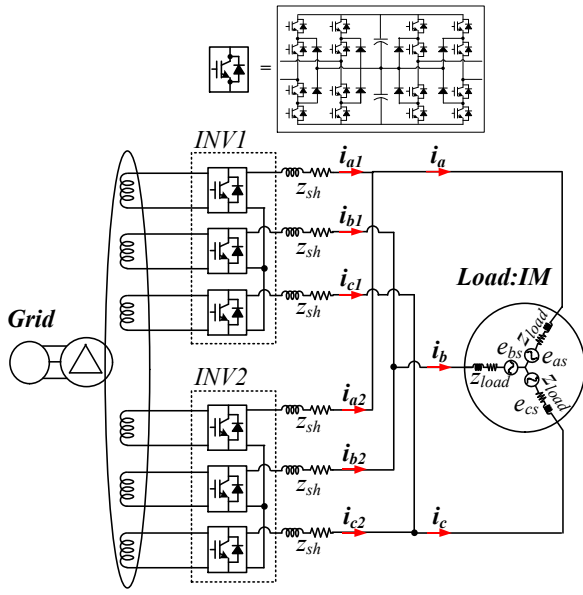
Fig.8 shows the experimental setup for verifying the proposed scheme to suppress the circulating current. Two parallel system ($n=2$) configuration with AFE 5L-CHB is shown in Fig.8 (a). This configuration has been implemented as shown in Fig.8 (b). The parameters of induction machine (IM) and

sharing inductor are listed in Table III. The induction machine is driven by V/F control and a DC motor (DCM) is used as load machine. DC-link voltage reference and switching frequency are 200V and 2.5 kHz, respectively.

Square of circulating current magnitude, $i_{cir_mag_sq}$, is defined as (16), by using stationary d, q-axis currents, i_{ds_cir} , i_{qs_cir} . This variable can be used as index of how much circulating current is reduced by proposed method because it represents the amount of total circulating current. Besides by using the value, RMS value of circulating current is easily calculated by (17).

$$i_{cir_mag_sq} = i_{ds_cir}^2 + i_{qs_cir}^2 \quad (16)$$

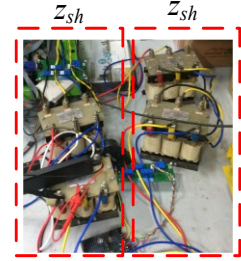
$$RMS = \sqrt{\text{average}(i_{cir_mag_sq})} \quad (17)$$



(a) circuit under experimental test



AFE 5level CHB



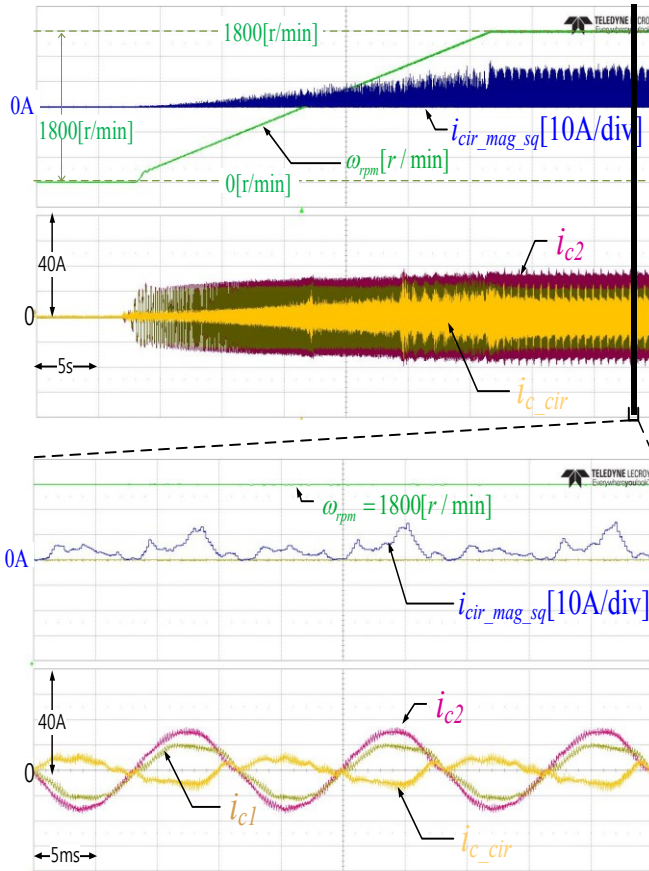
Sharing inductor



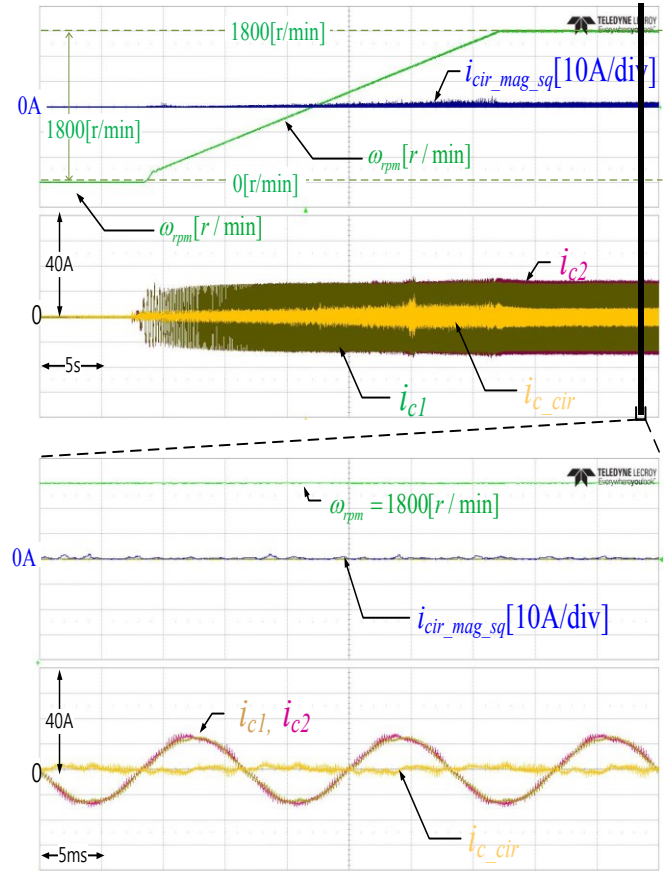
MG-set : IM&DCM

(b) experimental set-up

Fig. 8: experimental circuit and set-up under test



(a) without circulating current suppression control



(b) with circulating current suppression control

Fig. 9: Experimental results : Acceleration mode under no load condition

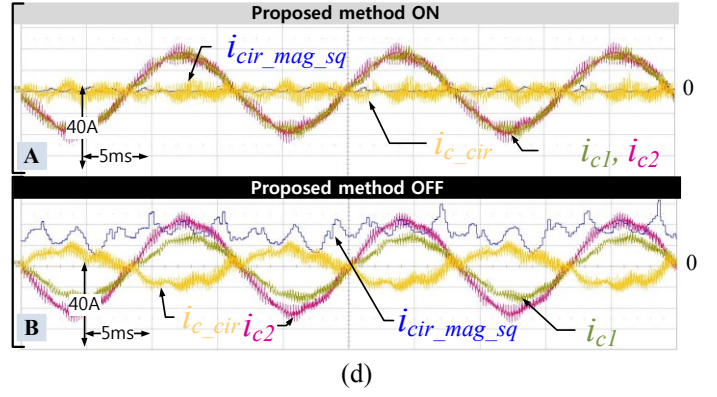
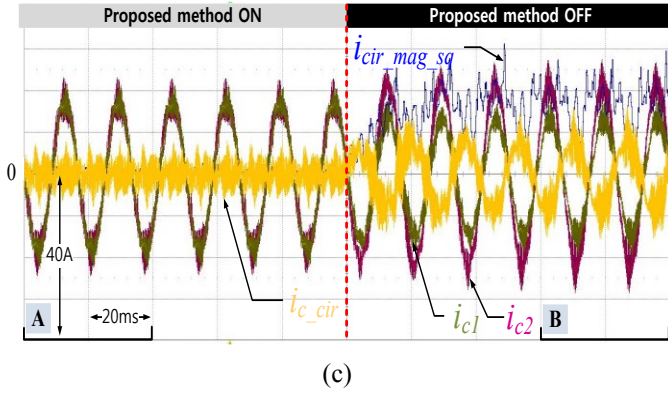


Fig. 10: Experimental results 2: steady state under 75% load condition at rated speed

TABLE III. EXPERIMENTAL PARAMETER

Parameter	Value
Rated power	11kW
Rated speed	377 rad/s
Pole number	4
Rated torque	58Nm
$L_{\sigma}(L_{ls}+L_{lr})$	2.4mH
Sharing inductor(Z_{sh})	2x40uH

Fig. 9 shows experimental results, when the machine is accelerated from standstill to the rated speed, under no load condition. In Fig. 9 (a), where circulating current is not controlled, the maximum circulating current is $3.9A_{peak}$, and its Root Mean Square (RMS) value calculated by (17) is $2 A_{rms}$. In Fig. 9 (b), where the proposed circulating current control method is applied, the maximum peak circulating current and its RMS are cut down to 8.8%, 33.7%, respectively.

Fig. 10 shows steady state waveform under 75% load condition at the rated speed. When the proposed method is engaged, RMS and maximum circulating current are $1.48A_{peak}$, $0.72 A_{rms}$, respectively. After the proposed scheme is disengaged, RMS and maximum circulating current reach $3.4A_{rms}$ and $5.7A_{peak}$, respectively. In other words, by employing the proposed method, RMS and maximum of the circulating current are decreased by 21.2% and 26% respectively.

It is demonstrated from above experimental results that under full load condition at the rated speed the drive system can operate well with much less circulating current through the proposed suppression method. The magnitude of voltage to control the circulating current is only below 3V, which 1.5% of the rated voltage of DC link. Also, the peak values of circulating currents are suppressed below under 2A, which is 3.6% of the rated load current, at any load. However, without the proposed control, the drive system fails under the same load condition, due to over current protection that limits the maximum current level of this system.

V. CONCLUSION

In this paper, the phenomenon regarding the circulating current flowing between inverters which have isolated dc-link such as Cascaded H Bridge (CHB) topology operating in parallel has been analyzed. A general circuit model to calculate the circulating current has been deduced from n paralleled inverter case. Based on this model, a scheme to suppress the circulating current has been proposed and implemented. Also, a guideline of the gain setting of the controller is presented. Finally, the validity, feasibility and effectiveness of the proposed method have been verified by simulation and experimental results. By using the proposed method, the circulating current of the drive system is not only suppressed effectively but also the drive system can be free from overcurrent fault due to the circulating current.

REFERENCES

- [1] J. L. Agorreta, M. Borrega, J. Lopez, and L. Marroyo, "Modeling and control of N-paralleled grid-connected inverters with LCL filter coupled due to grid impedance in PV plants," IEEE Trans. Power Electron., vol. 26, no. 3, pp. 770–785, Mar. 2011.
- [2] F. Bovolini and H. Pinheiro, "Flexible arrangement of static converters for grid connected wind energy conversion systems," IEEE Trans. Ind. Electron., vol. 61, no. 9, pp. 4707–4721, Sep. 2014.
- [3] Z. Ye, D. Boroyevich, J. Y. Choi, and F. C. Lee, "Control of circulating current in two parallel three-phase boost rectifiers," IEEE Trans. Power Electron., vol. 17, no. 5, pp. 609–615, 2002.
- [4] R. Li and D. Xu, "Parallel operation of full power converters in permanent-magnet direct-drive wind power generation system," IEEE Trans. Ind. Electron., vol. 60, no. 4, pp. 1619–1629, Apr. 2013.
- [5] S. K. Mazumder, "Continuous and discrete variable-structure controls for parallel three-phase boost rectifiers," IEEE Trans. Ind. Electron., vol. 52, no. 2, pp. 340–354, Apr. 2005.
- [6] C. T. Pan and Y. H. Liao, "Modeling and coordinate control of circulating currents in parallel three-phase boost rectifiers," IEEE Trans. Ind. Electron., vol. 54, no. 2, pp. 825–838, Apr. 2007.
- [7] C. T. Pan and Y. H. Liao, "Modeling and coordinate control of circulating currents for parallel three-phase boost rectifiers with different load sharing," IEEE Trans. Ind. Electron., vol. 55, no. 7, pp. 2776–2785, Jul. 2008.
- [8] T. P. Chen, "Circulating zero-sequence current control of parallel three-phase inverters," IEE Proceedings-Electric Power Appl., vol. 153, no. 2, pp. 282–288, 2006.

- [9] T. P. Chen, "Dual-modulator compensation technique for parallel inverters using space-vector modulation," *IEEE Trans. Ind. Electron.*, vol. 56, no. 8, pp. 3004–3012, 2009.
- [10] Z. Shao, X. Zhang, F. Wang, and R. Cao, "Modeling and Elimination of Zero-Sequence Circulating Currents in Parallel Three-Level T-Type Grid-Connected Photovoltaic Inverters," *IEEE Trans. Power Electron.*, vol. 30, no. 2, pp. 1050 – 1063, 2015.
- [11] J. S. S. Prasad, R. Ghosh, and G. Narayanan, "Common-Mode Injection PWM for Parallel Converters," *IEEE Trans. Ind. Electron.*, vol. 62, no. 2, pp. 789–794, 2015.